ELSEVIER

Journal of Experimental Marine Biology and Ecology
243 (2000) 55–80

JOURNAL OF EXPERIMENTAL MARINE BIOLOGY AND ECOLOGY

www.elsevier.nl/locate/jembe

Implications of brine channel geometry and surface area for the interaction of sympagic organisms in Arctic sea ice

C. Krembs[a,*], R. Gradinger[b], M. Spindler[b]

[a]*University of Washington, School of Oceanography, Box 357940, Seattle, WA 98195, USA*
[b]*Institut für Polarökologie, Wischhofstr. 1–3, Geb. 12, 24148 Kiel, Germany*

Received 25 April 1998; received in revised form 22 July 1999; accepted 23 July 1999

Abstract

Dynamic temporal and spatial changes of physical, chemical and spatial properties of sea ice pose many challenges to the sympagic community which inhabit a network of brine channels in its interior. Experiments were conducted to reveal the influence of the internal surface area and the structure of the network on species composition and distribution within sea ice. The surface of the brine channel walls was measured via a newly developed method using a fluorogenic tracer. These measurements allowed us to quantify the internal surface area accessible for predators of different sizes, at different ice temperatures and in different ice textures. Total internal surface area ranged from 0.6 to 4 m^2 kg^{-1} ice and declined with decreasing ice temperature. Potentially, 6 to 41% of the area at -2°C is covered by micro-organisms. Cooling from -2 to -6°C drastically increases the coverage of organisms in brine channels due to a surface reduction. A combination of brine channel frequency measurements with an artificial brine network experiment suggests that brine channels ≤ 200 μm comprise a spatial refuge with microbial community concentrations one to two magnitudes higher than in the remaining channel network. The plasticity of predators to traverse narrow passages was experimentally tested for representative Arctic sympagic rotifers, turbellarians, and nematodes. By conforming to the osmotic pressure of the brine turbellaria match their body dimensions to the fluctuating dimensions of the brine channel system during freezing. Rotifers penetrate very narrow passages several times their body length and 57% their body diameter. In summary, ice texture, temperature, and bulk salinity influence the predatory–prey interactions by superimposing its structural component on the dynamic of the sympagic food web. Larger predators are excluded from brine channels depending on the architecture of the channel network. However, extreme body flexibility allows some predators to traverse structural impasses in the brine channel network.

Keywords: Adaptation; Internal surface; Sea ice; Patchiness; Predation; Refuge space

*Corresponding author. University of Washington, School of Oceanography, Box 357940, Seattle, WA 98195, USA.
E-mail address: ckrembs@ocean.washington.edu (C. Krembs)

0022-0981/00/$ – see front matter
PII: S0022-0981(99)00111-2

1. Introduction

Sea ice covers large parts of the polar seas all year round (Maykut, 1985) and is colonised by a diverse sympagic (= living with ice, Horner et al., 1992) community, which includes bacteria, fungi, algae and proto- and metazoans (Horner, 1985, 1990). Void spaces inside the ice that can be colonised are composed of a highly interconnected brine channel system which develops during the formation of ice. Brine channel diameters span from several micrometres to several centimetres (Weissenberger, 1992; Eicken et al., 1995). Resin cast studies (Weissenberger et al., 1992) of Antarctic sea ice visualised the very complex three-dimensional structure of the brine channel system. Changes in geometry of the brine channels occur in concert to physical fluctuations and ion composition. The volume of brine changes in relation to temperature and bulk salinity of the ice (Frankenstein and Garner, 1967; Leppäranta and Manninen, 1988), whereas brine salinity exclusively follows ice temperature (Assur, 1958).

The spatial distribution of sympagic organisms is highly variable on vertical (Horner, 1985) and horizontal (Spindler and Dieckmann, 1986) scales, which is attributed to light conditions, salinity, temperature, ice texture, ice formation (Cota and Horne, 1989; Eicken, 1992), nutrient availability (Cota et al., 1987) and trophic interactions.

Brine channel walls constitute large surface areas that can be colonised by sympagic organisms and used as sites for attachment, locomotion, and grazing. Many ice-inhabiting organisms are considered to manifest distinct surface affinities, including bacteria (e.g., Smith et al., 1989), pennate diatoms (e.g., Sullivan and Palmisano, 1984), protozoans (e.g., Spindler and Dieckmann, 1986; Agatha et al., 1990; Ikävalko and Gradinger, 1997) and metazoans (Andriashev, 1968; Carey, 1985; Spindler et al., 1990; Gradinger et al., 1991).

From sediment, soil and hard rock substrates it is known that substrate structure can strongly influence biological interaction (e.g., Fenchel, 1969; Elliott et al., 1980; Menge et al., 1985; Patterson et al., 1989; Van Veen and Kuikman, 1990; England et al., 1993; Paul et al., 1994). For soils it was speculated that increased bulk densities negatively affect the accessibility of pore space for meso- and macrofauna (Soane et al., 1982) and reduce the predatory activity of protozoa and nematodes on bacteria and fungi. For marine sediments a ‘critical grain size’ of about 200 μm for most metazoa (Jansson, 1967; Fenchel, 1969), 120 μm for ciliates and several tens of micrometres for flagellates and amoeba have been suggested (Lighthart, 1969; Alongi, 1987).

Brine volume and crystal structure of marine ice finds its analogy in water content and texture in soils which are key variables defining colonisable space in the latter habitat (Smiles, 1988). Similar to observations in soils and aquatic sediments (Patterson et al., 1989) we assume that accessible pore space plays an important role for the geochemical cycling and biological interaction in marine ice as suggested by Eicken (1992). Internal surface area has long been used as an important substrate parameter for aquatic sediments (De Flaun and Mayer, 1983; Yamamoto and Lopez, 1985), but reports on sea ice are not available to date.

In our paper we present first evidence for the influence of brine channel geometry on the interaction of predator and prey in sea ice via size-specific predator exclusion experiments in an artificial ice substrate. A new method (the rhodamine chloride

adsorption method, RCA) is described to determine the internal surface of sea ice. Detailed control experiments were carried out to ensure its accurate application and are therefore incorporated into the Material and methods section of the publication.

The combination of several experiments allows us to address the following questions:

1. How large is the entire internal surface of sea ice and which fraction of this surface is accessible for organisms of different sizes?
2. How does temperature control the accessible pore space and consequently the distribution of organisms inside sea ice?
3. Are organisms distributed equally inside all accessible brine channels?
4. Does the brine channel geometry influence the trophic interactions of the sympagic community?

2. Material and methods

Two different methods were devised in order to answer the above raised questions. The first measures the total surface area of brine channel walls via the adsorptive property of a fluorogenic dye to ice. For this method detailed experiments were carried out to evaluate its correct application which then allowed us to allocate wall surface area to brine channels of different diameters. The second method tested how a mixed population of ice-inhabiting organisms behaved and colonised an artificial substrate that simulated the wide size range of brine channel diameters which sympagic organisms encounter in their natural habitat. Observations on the behaviour of predators to increased salinities and narrow brine channel passages are described to evaluate their potential to traverse impasses in the brine channel network under a range of environmental conditions.

2.1. Methodological development of the rhodamine chloride adsorption method

In three experiments we tested the dynamics of the adsorption of the fluorogenic dye rhodamine chloride to ice surfaces.

2.1.1. General sample treatment

For the determination of brine channel surfaces we used the fluorochrom rhodamine chloride (RC, Basic Red 1, Sigma) which can be detected at very low concentrations due to its fluorogenic properties. For calibration we measured the fluorescence of a known RC concentration with a SFM 25 Kontron Instrument fluorometer (excitation wavelength 440 nm, emission wavelength 550 nm). The adsorption of RC to ice surfaces was determined using freshwater ice disks of known surfaces (24.7 cm^2) and 10 different RC concentrations (Table 1). For each experiment three replicate pieces of ice were used. Ice pieces were submersed and stirred in a saline RC solution simulating natural brine of

Table 1
Experimental setup for adsorption experiments of rhodamine chloride (RC) in a salty solution

Exp. No.	RC concentration (μg RC m1^{-1})	Salinity	Temperature (°C)
1	Salinity/RC = 630.34 (0.05–0.23)	40.9, 52.7, 65.7, 80.0, 93.9, 114.6, 133.1, 142.7	−2.3, −3.1, −3.8, −4.7, −5.6, −7.1, −8.3, −9.1
2	0.00–0.15 (Fig. 1)	17.4	−1.0
3	0.55	67.7	−3.9

sea ice for 1 min and then taken out with tweezers. Drops were carefully removed and ice pieces were melted for further analysis. Dye concentration was measured fluorometrically. Volumes of melted ice pieces were determined gravimetrically (accuracy $\pm 10^{-4}$ g). The mass of RC that adsorbed to the ice was calculated by multiplying the RC concentration by the volume of the melted ice and relating it to the initial surface of the ice piece.

Salinity and temperature of the saline RC solution (Table 1) were measured with a WTW LF 325 probe. To avoid freezing and melting of ice, which potentially interferes with the adsorption of RC, water and ice were critically kept at thermodynamic equilibrium (Assur, 1958) using dewars and extra ice pieces that floated freely inside the water. Water was continuously stirred to guarantee a homogeneous distribution of solutes and temperature.

2.1.2. Calibration of the RCA method to ice surfaces under simulated in situ conditions of salt and temperature

In the first experiment salt and RC were used in a fixed ratio (salinity/RC = 630.34) to simulate the synchronous increase of salt and dye concentration which naturally occurs when ions are rejected from the ice matrix during freezing of sea ice. In a second experiment only the concentration of RC was raised from 0 to 0.15 mg ml^{-1} at a constant temperature (−1.0°C) and salinity (17.4).

As a control for adsorption biases of RC to the wall surface of the polystyrene tissue culture dishes, in which ice pieces had been melted, we rinsed them thoroughly with 1 ml acetone (90%) which was demonstrated to be a good solvent. RC concentration was measured fluorometrically in acetone. Errors due to adsorption accounted for less than 1% of the bulk water concentration and were therefore neglected for all further calculations.

Fig. 1 shows the linear relations between RC concentration in the water and adsorbed RC under the two experimental conditions. Adsorbability was not significantly different, indicating that the adsorption of RC to the ice surface primarily depends on the RC concentration in our investigated range.

2.1.3. Adsorption velocity of RC to ice

The adsorption of RC to ice is time dependent and was assumed to follow the mathematical model of Michaelis–Menten at thermodynamic equilibrium. To determine the saturation constant of RC towards ice surfaces experimentally, the protocol (described above) was expanded using different submersing times at a salinity of 67.7

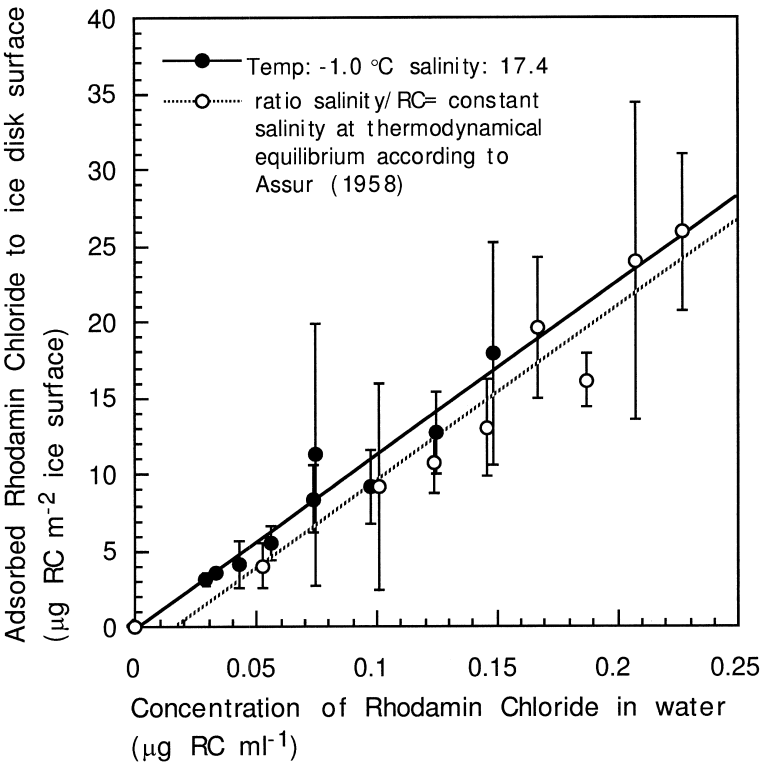

Fig. 1. Concentration-dependent adsorption of rhodamine chloride (RC) to freshwater ice surfaces tested in water with varying salinity and temperature.

and RC concentration of 0.55 mg ml^{-1}. The minimal required adsorption time was approx. 40 s to achieve 99% of the adsorption of RC.

2.1.4. Test of the resolution of the RCA method

We tested whether the RCA method allows a determination of ice surfaces by comparing RCA measured ice surfaces to freshwater ice pieces of known surface area. Ice pieces with different surface areas were dipped into sea water containing RC (0.11 mg ml^{-1}, salinity 17.4, temperature at thermodynamic equilibrium of -1.0°C) and stirred for 1 min. Then the ice was melted and analyzed for fluorogenic dye and salt content, following the protocol described above.

To calculate the surface of the ice from the adsorbed amount of RC the empirical formula (1) (based on data in Fig. 1) was used:

$$A_i = \frac{c\mathrm{RC}_i \cdot V_i}{(a \cdot c\mathrm{RC}_w + b)},\ a = 1.1413 \times 10^{-2}\ (\mathrm{cm}),$$
$$b = -1.7268 \times 10^{-4}\ (\mu\mathrm{g\ RC\ cm}^{-2}) \quad (1)$$

were A_i is the surface of ice (cm^2), cRC_i the concentration of RC in the melted ice (μg RC ml^{-1}), V_i the volume of the melted ice (ml), and cRC_w the concentration of RC in water (μg RC ml^{-1}). The constants a and b were determined from the adsorption of known RC solutions to a known ice surface (Fig. 1). Fig. 2a illustrates the accuracy of the RCA method to measure ice surfaces with a mean relative residuum of 7%.

Having quantified the principle of operation and accuracy of the RCA method we applied the method to sea ice. First we quantified the rejection of RC from the ice matrix during the formation of sea ice. In a second step we ascertained that brine was completely separate from the ice matrix, which is critical for the quantification of internal ice surfaces.

2.2. Determination of RC incorporation during ice formation

In further experimental tests we determined the RC expulsion from growing ice. As a first model we used freshwater ice formation, where dissolved ions are rejected from the ice matrix during ice growth (Martin, 1981; Fang et al., 1984) and also to omit the difficulties which are encompassed in sea ice by liquid entrapment in isolated brine pockets.

Distilled water was frozen at different ice formation rates (0.03–0.80 cm ice h^{-1}) in 10 l insulated buckets containing RC concentrations ranging from 0.03 to 0.69 μg ml^{-1}. Ice thicknesses were measured in regular intervals with venire callipers. Average freezing rates were determined when the ice had reached approx. 5 mm thickness. Ice sheets were removed from the bucket and rinsed briefly (2 s) under 10°C running tap water to liberate the ice from adhering water droplets containing dissolved and adsorbed RC. Cleaned ice sheets were melted and the RC concentration was measured fluorometrically. The ratio of RC concentration in solution to the concentration in the ice was used to calculate the freezing-rate-dependent incorporation of RC (Fig. 2b), which exhibited low values at low freezing rates.

2.2.1. Centrifugation of ice cores

Centrifugation of ice core segments is a tool for collecting the brine from the brine channel network (Weissenberger et al., 1992). We used a chilled centrifuge at 1500 r.p.m. for 20 min (Centricon T-324, Kontron Instruments) at approx. 1 K below their original temperature. To evaluate whether the centrifugation procedure sufficiently separated brine from the ice, five cores with a temperature of -3.4°C were centrifuged for 0, 1, 2, 5 and 20 min at a temperature of -4.6°C. The amount of collected brine was measured gravimetrically and related to the weight of the centrifuged ice cores. Highest brine expulsion rates occurred during the first 2 min (data not shown) and half of the drainage of the ice core occurred after 19 s. No additional brine was obtained after 5 min, which was chosen as the minimum centrifugation time.

2.3. Application of the RCA method

The internal surface area of interconnected brine channels was determined for

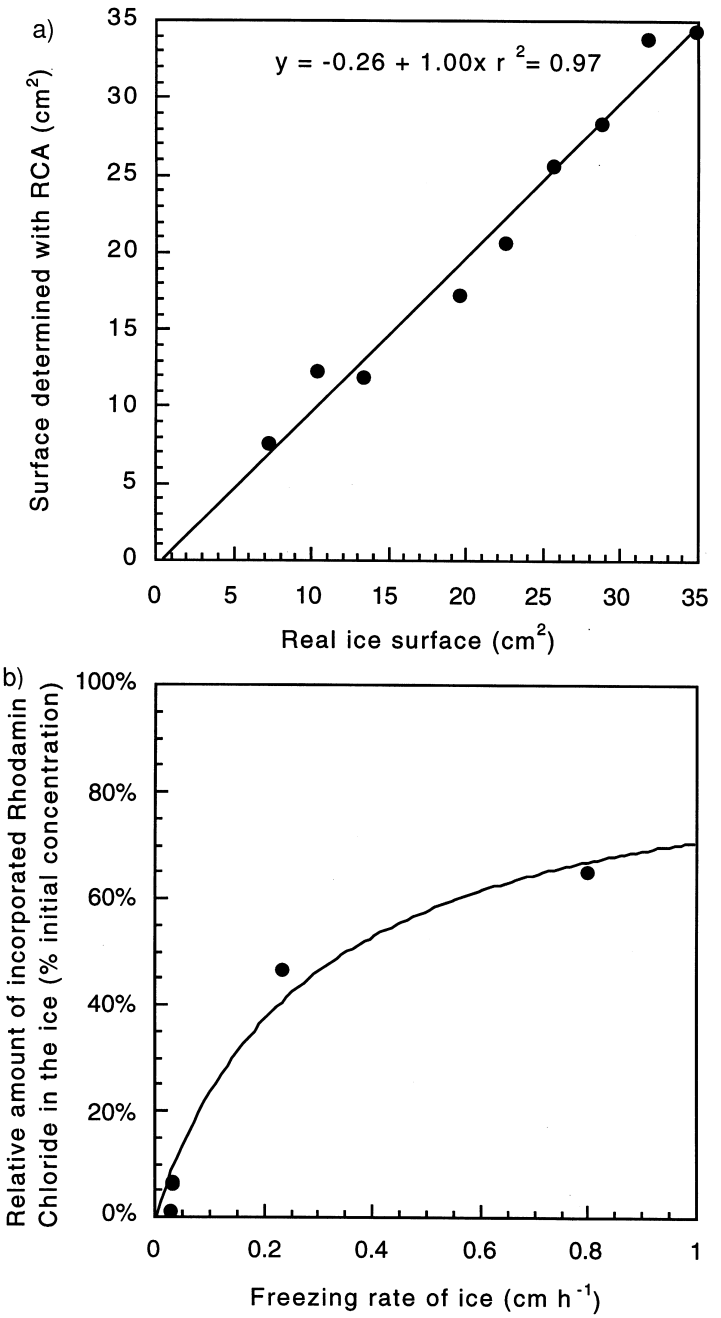

Fig. 2. (a) Surface determination of freshwater ice with the RCA method tested against defined ice surfaces (RC concentration, 0.11 μg ml^{-1}; *S*, 17.4; *T*, −1.0°C). (b) Freezing-rate-dependent incorporation of rhodamine chloride into freshwater ice.

columnar and granular ice (Lange and Eicken, 1991) at various temperatures, for which the frequencies of brine channel diameters and their relative contribution to the total internal ice surface were also determined.

2.3.1. Surface of interconnected brine channel walls in artificial sea ice at different temperatures

The surface area of brine channels was determined for columnar ice at temperatures between −2.2 and −6.1°C. Ice was formed in a polyethylene container (60×41×40 cm) at −20°C from artificial sea water (Instant Ocean, salinity 33.3) to which RC (0.06 μg ml^{-1}) was added. Freezing rates were determined by repetitive measurements of the ice thickness. After the ice had reached a thickness of 10 cm, three replicate ice cores were collected with an ice corer (5 cm diameter) for the surface determination. One extra core was sampled for the analysis of the frequency of brine channel diameters. The upper 2 cm of the ice cores were discarded. Ice cores were fitted into plastic jars of similar diameter, sealed with screw caps and placed upside down. Cores were equilibrated to temperatures of −2.2, −3.1, −4.1, −5.2 and −6.1°C for 12 h. Upside down positioned jars reduced the brine drainage from the ice. For brine collection, ice was centrifuged at 1500 r.p.m. for 20 min at 1° below their original temperature. Brine and centrifuged ice cores were brought separately to room temperature. Brine volume was determined gravimetrically (accuracy 10^{-5} g). Salinity of the brine and the melted ice was measured with a WTW 325 probe. RC concentration was determined fluorometrically. Both concentrations were converted to weight of RC and salt, respectively.

In a second experiment granular ice was produced from the same artificial sea water. Water was agitated with three magnetic stirrers placed at even distances into the containment. Freezing was initiated at −20°C. After an approximately 5 cm thick frazil ice layer had developed at the surface, plastic jars were filled with ice slush and brought to temperatures of −2.9, −3.6, −5.8 and −6.8°C during 24 h. Temperatures differed from the frazil ice experiment due to technical limitations. When the ice slush had consolidated the frozen ice samples were treated similar to columnar ice.

2.3.2. Calculation of surfaces of interconnected brine channels

Internal ice surfaces were calculated via the ratio of salt to RC in both brine and emptied ice cores:

$$\frac{S_1}{S_2} = \frac{R_1 + x}{R_2 - x} \tag{2}$$

where S_1 and R_1 are the weight of salt and RC in the brine and S_2 and R_2 represent the weight of salt and RC in the melted remaining ice after centrifugation. Parameter x gives the weight of RC adsorbed to the brine channel walls. Brine that remains in sealed pockets after centrifugation follows the above equation with $S_1 = S_2$ and $R_1 = R_2$ and $x = 0$ upon melting. Consequently, only the surface of open interconnected channels was measured. By relating the weight of adsorbed RC to unit area surface of brine channel walls A_i (cm^2):

$$A_i = \frac{x}{(a \cdot cRC_b + b)},\ a = 1.1413 \times 10^{-2}\ (\text{cm}),$$
$$b = -1.7268 \times 10^{-4}\ (\mu\text{g RC cm}^{-2}) \quad (3)$$

where cRC_b (μg RC ml^{-1}) is the concentration of RC in the brine and a and b are empirical constants of Eq. (1).

2.3.3. Frequency of brine channel diameters

Thin sections of ice cores were made following Lange and Eicken (1991). Sections were cut parallel to the freezing direction. Thin sections (1 mm thickness) were mounted onto glass slides and video pictures were taken from fields along three parallel transects spanning the entire length of the core. Ice structures were analysed under a polarised light microscope (Leitz Orthoplan) at a final magnification of 220× and a temperature of −30°C. Video pictures were analysed on a Next Computer using the image analysis program BILD (W. Hukriede, Kiel, Germany). The frequency distribution of brine channel diameters is a combined estimate of the brine channel sizes and their relative concentration because diameters of brine channels were measured at each intersection between brine channel outline and an evenly spaced grid (size 83 μm). Measurements were conducted across the shortest channel diameter with a minimum of 2×10^3 measurements for each ice core.

2.3.4. Allocation of internal ice surface area to brine channels of certain diameters

Based on the frequency distribution of brine channel diameters for each ice sample, measured surface areas were allotted to different brine channel size classes assuming that all brine channels combined must equal 100%. Brine channel diameters were converted to circumferences of brine channels assuming a circular cross section. The frequency distribution of brine channel circumferences was fitted to a forth-order polynomial function (BC) via the least square method.

2.3.5. Internal surface area accessible for predators of certain size

The maximal theoretical internal surface area (SA) that a predator can traverse inside the ice at a given temperature (neglecting the presence of obstructing passages) is bound to its plasticity of body circumference. SA was calculated by numerically integrating the function *BC* beginning at the diameter of the predator *cp* to the largest brine channel that was encountered (*lbc*):

$$\text{SA} = \sum_{cp}^{lbc} BC$$

2.4. Behaviour and colonisation of organisms inside an artificial brine channel network

2.4.1. Changes of predator size with salinity

Turbellaria are frequently occurring sea ice metazoans which are poikiloosmotic (Penzlin, 1981). During cooling of sea ice the salinity in the brine increases (Assur,

1958) while brine volume decreases (Frankenstein and Garner, 1967). To test whether turbellarian body dimensions comply with a salt increase and a reduction of brine channel diameter during cooling, animals (obtained during the expeditions ARK XI/1 and ARK XIII/1 on board *R.V. Polarstern*) were gradually exposed to increasing salinities ranging from 10 to 85 at +4°C. Acclimation time to each condition was 1 day. Based on video recordings of actively moving animals their body width and length was determined using the same image analysis system as above.

2.4.2. Capillary experiment

Glass capillaries of various diameters served as model substrates to mimic the brine channel habitat of sea ice. Pasteur pipettes were manufactured with a Bunsen burner with diameters ranging from several to hundreds of micrometres which were sized and selected using a Wild M8 Binocular. Capillaries were broken into approximately 5–10 mm long pieces and aged in 0.08% HCl for 3 days. Capillaries were rinsed five times with filtered sea water and aged for an additional 14 days. Capillaries of different sizes were placed in tissue culture dishes (ø 35 mm) that contained cultures of ice organisms obtained from the Laptev Sea ice during the expeditions ARK XI/1 and ARK XIII/1 with the *R.V. Polarstern*. Cultures contained copepods, rotifers, nematodes, ciliates, flagellates, amoebae, diatoms and bacteria in varying proportions. Four replicas containing glass capillaries with diameters ranging from 12 to 1420 μm were incubated for 3 weeks at 4°C at light/dark cycles of 6 h:6 h and a light intensity of approx. 1.5 μE m^{-2} s^{-1}. Cultures were surveyed each day with a Wild M8 Binocular (magnification 20×, 40×, 80×) and a Zeiss microscope at 200×. A video camera (Panasonic F15 HS) mounted to the binocular and the microscope allowed us to film the movement of organisms inside the capillaries and the culture dish. To control for changes in the abundance of predators (copepods, rotifers, nematodes, ciliates) outside the capillaries 28.3% of the volume of the culture dishes was counted every second day. Recounted fields ($n = 15$) shortly after one another rendered a maximal sampling error of 25% for these counts. The experiment was terminated after 24 days by adding glutaraldehyde (final concentration 4%) to the water. The fixation process was observed under the binocular to ensure that organisms were fixed properly and did not leave the capillaries. Abundances of organisms inside the capillaries were determined with a Zeiss inverted microscope at a magnification of 200×. The detection limit of organisms inside the capillaries was approx. 4 μm due to the optical distortion imposed by the capillary walls. Capillaries with diameters >1000 μm could not be analysed at this magnification and were therefore left out.

To determine the body diameter of the organisms, randomly picked individuals were video-taped and sized with the computer aided image analysis system. Concentrations of organisms per capillary were calculated by converting capillary diameters and length to volume and surface area, respectively.

To assess the flexibility of predators to move inside narrow geometries of the ice we tested the ability of animals to pass through very thin round bottlenecks in our model substrate. Glass capillaries of 5 mm diameter decreased conically towards one end at a rate of 0.078 (mm mm^{-1}) to a terminal orifice of 69 μm. The capillary was positioned in prefiltered sea water such that the narrow end was submersed and the large opening

faced out of the water. This allowed only one direction for the organisms to leave the capillary. In several repetitive experiments single amphipods, harpacticoid copepods, rotifers and ciliates were introduced into the capillary via the larger opening. Their movement was followed and recorded by the optical system described above until they either left the capillary system or became stuck in the narrowing end. Minimal diameters that were successfully traversed were measured.

3. Results

3.1. Application of the RCA method

3.1.1. Surface of brine channel walls in artificial sea ice at different temperatures

Ice which was quietly frozen consisted predominantly of columnar ice with crystal length between 1 and 2 cm; granular ice consisted of very small crystals (1–7 mm). Calculated theoretical brine volumes and salinities (Assur, 1958; Frankenstein and Garner, 1967) for different temperatures are presented in Fig. 3 together with our measured data. More brine could be extracted from columnar than from granular ice (ratio of extracted brine volume to theoretical brine volume: median 0.63, $n = 5$ for columnar ice; median 0.49, $n = 5$ for granular ice).

Columnar ice formed at a rate of 0.075 cm h^{-1}. Melted 8 cm thick columnar ice pieces had a bulk salinity of 14.9, which corresponds to 44.9% of the initial salinity of the water. Surface area (Fig. 4a) determined with the RCA method ranged from 0.1 to 7.2 m^2 kg^{-1} ice and decreased exponentially with decreasing temperature. Melted granular ice had a bulk salinity of 28.7, which corresponds to 86.2% of the initial water salinity. Surface area ranged between 0.3 and 0.7 m^2 kg^{-1} ice with a decrease towards lower temperatures (Fig. 4b).

3.1.2. Frequency distributions of brine channel diameters of artificial sea ice and allocation of total internal surface area to brine channels of given diameters

Frequency distributions of brine channels converted to total internal surface for both ice types are illustrated in Fig. 5a. The smallest channels contributed to the highest proportions of the total surface area in both ice types (Fig. 5b). Their relative contribution increased with decreasing temperature. The partitioning of surface area in columnar ice differed slightly from granular ice at higher temperatures. Granular ice showed a higher fraction of brine channels of 0 to 21 μm in cold ice (< -5.8°C). A difference between both ice types occurred in the relative contribution of brine channel surface with diameters between 62 and 165 μm: in columnar ice their contribution increased at lower temperatures, granular ice was less affected by temperature.

3.1.3. Internal surface area accessible to predators

The maximal surface area that an organism of a given diameter can traverse was calculated from the frequency distribution of brine channels. Fig. 6 demonstrates the reduction of accessible surface space expressed as total available surface for tempera-

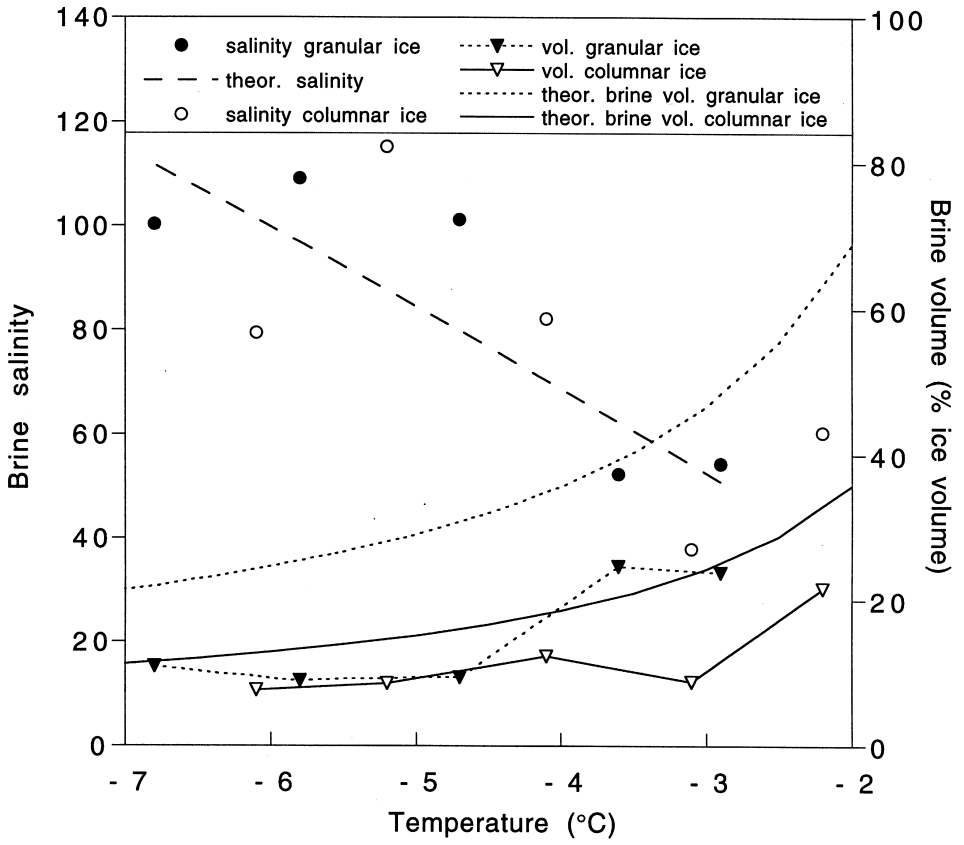

Fig. 3. Comparison of theoretical vs. measured values of brine salinity and brine volume for ice cores used to determine internal surfaces and brine channel diameter frequency distributions (theoretical salinity after Assur (1958), theoretical values of brine volume after Frankenstein and Garner (1967)).

tures around −2.5°C for both ice types. The relative accessible surface area for predators of a given diameter did not vary significantly for both ice types at temperatures between −2.2 and −6.8°C.

3.2. Capillary experiment

Capillaries were colonised in all four replicate experiments. The range of inner diameters of glass capillaries covered the majority of diameters of brine channels that are found in sea ice (Fig. 7). Capillaries were grouped into size classes to determine their content of organism (Fig. 7a). Measured body widths of dominant organism taxa found in the cultures from the Laptev Sea are shown in Fig. 8a,b.

During the 24 day incubation, changes in organism abundance occurred (Fig. 9) due to organism growth (ciliates, amoeba) and mortality (copepods, rotifers). Inside the capillaries the presence of certain taxa was sporadic and irregular (nematodes, copepods,

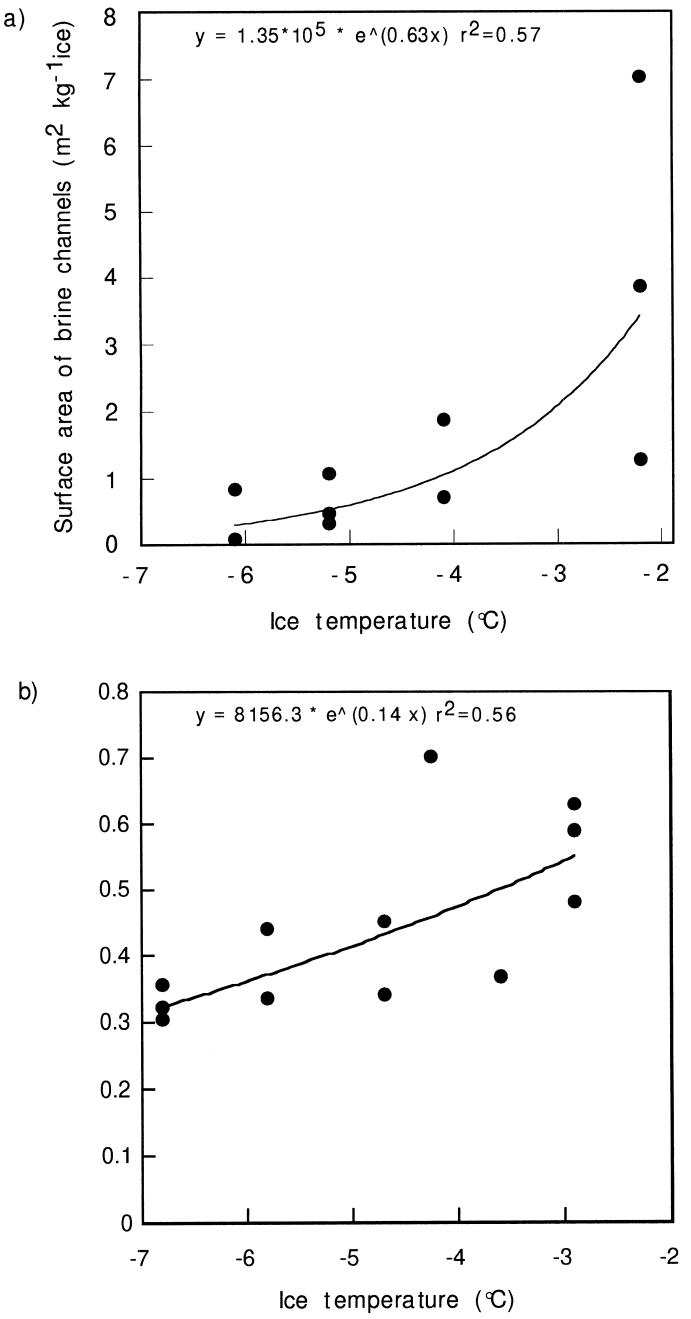

Fig. 4. Exponential decrease of surface area of artificial sea ice measured with the RCA method for temperatures between −2.2 and −6.1°C for (a) columnar ice and (b) granular ice of −2.8 to −6.9°C. Columnar ice: initial water salinity 33.3, bulk salinity of ice 14.9. Granular ice: initial water salinity 34, bulk salinity of ice 28.7.

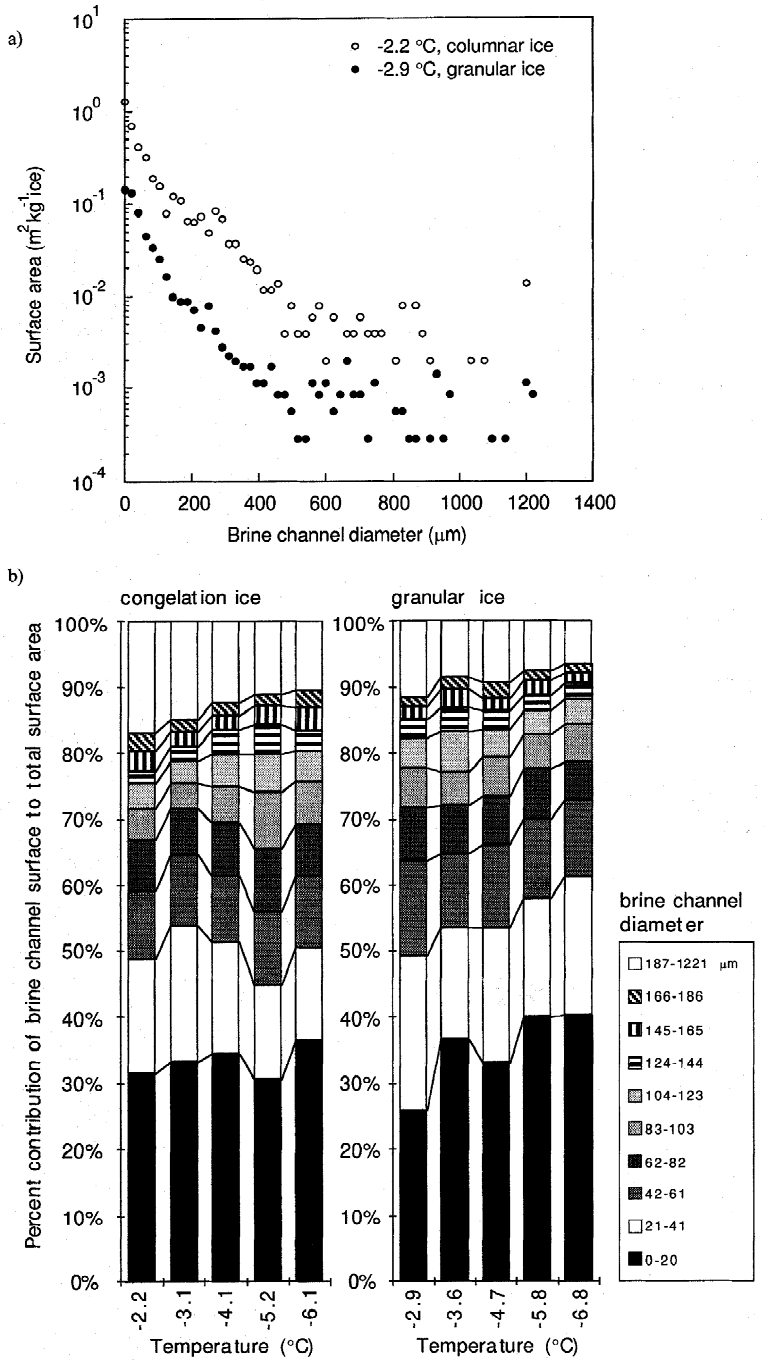

Fig. 5. (a) Absolute contribution of wall surface area of brine channels for columnar and granular ice. (b) Relative contribution of brine channels of different diameters to total internal surface at temperatures between −2.2 and −6.1°C for columnar ice and between −2.9 and −6.8°C for granular ice.

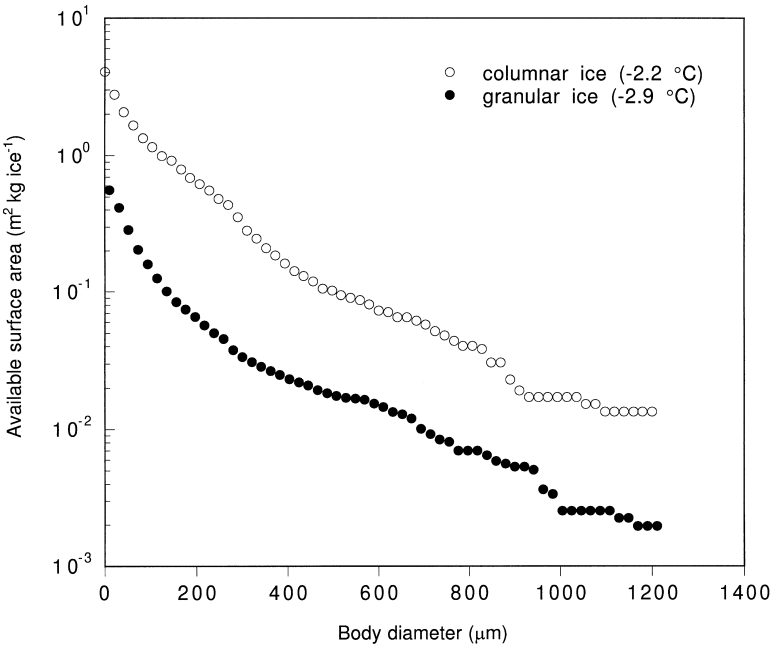

Fig. 6. Maximal available brine channel surface area for predators of a given body diameter for sea ice of approx. −2.5°C and different ice texture.

unidentified cysts) and did not follow a trend, however rotifers, ciliates and flagellates were frequently found inside capillaries with a maximum at day 24. An example of their concentration change inside the capillaries in relation to the concentration in the tissue dish is shown in Fig. 10.

During the experiment motile organisms entered and left the capillaries. Their averaged abundance for each capillary size class during the experiment is illustrated in Fig. 11. Organisms were absent in capillaries which were too small, but had their maximum abundance in capillaries which were only slightly larger than the organisms.

After an incubation of 24 days, organisms were counted inside the capillaries (Fig. 12). The abundance of species inside narrow capillaries was three orders of magnitude higher than in large capillaries. Minimal capillary diameters in which taxa still occurred were 12 μm for pennate diatoms, flagellates, ciliates and amoebae, 32 μm for cysts, 42 μm for rotifer and diatom chains and 102 μm for centric diatoms.

The observed minimum capillary diameters that were traversed as percent of the organism body diameter are summarised for selected motile animals in Table 2. Only rotifers and turbellaria traversed impasses significantly smaller than their normal body diameter, which they achieved by stretching and flexing their bodies.

The percent reduction in body diameter of acoel turbellaria in relation to ambient salinity is illustrated in Fig. 13. Turbellaria could reduced their initial body diameter by 70% compared to a salinity of 33. At low salinities (<30) body diameters varied greatly in diameter and higher salinities (>85) killed the animals. Length-to-width proportions

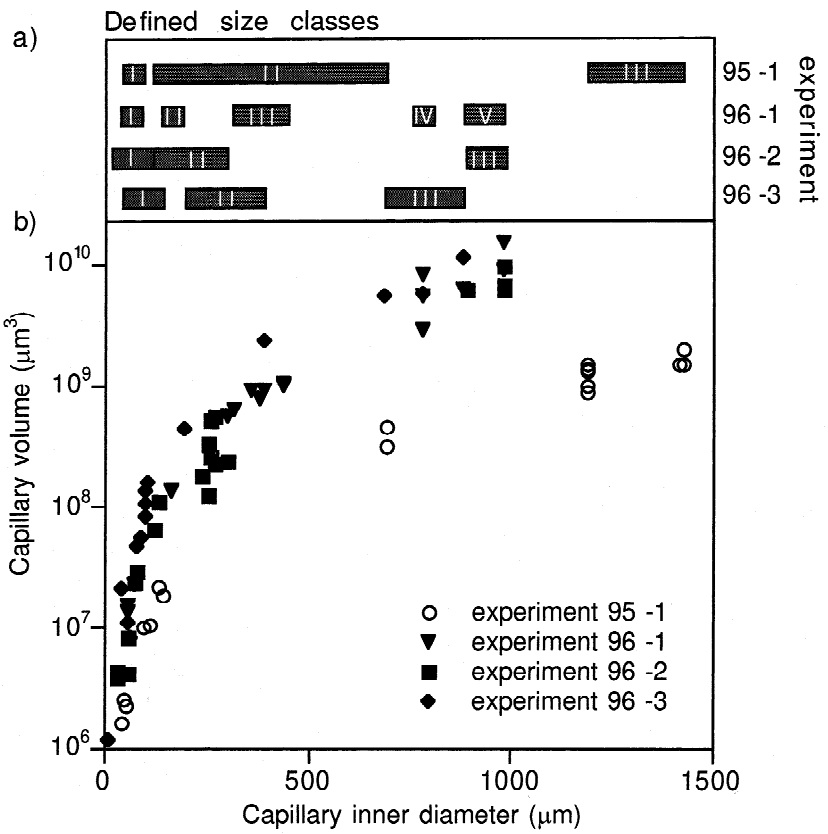

Fig. 7. Description of model substratum which simulates brine channels of various sizes. (a) Capillaries grouped into size classes. (b) Capillary volumes and diameters from four replicated experiments.

of the animals for all salinities tested can be expressed as length = 47.2 + 2.8*body diameter (μm) ($r^2 = 0.94$, $n = 65$), which shows that the animals change their body dimensions during osmotic stress to equal parts.

4. Discussion

The physical and chemical properties governing the sea ice brine channel system are predominant in the development of a sympagic community (e.g., Cota et al., 1991; Eicken, 1992). While many parameters, such as, for example, ice texture, brine temperature, salinity, volume or in situ nutrient concentrations, are determined during field work, the surface of the brine network remains unknown, despite its significance to many ice-inhabiting organisms (e.g., Ikävalko and Gradinger, 1997). Our rhodamine chloride absorption technique (RCA method) now allows the quantification of the ice surfaces of interconnected brine channels. However, measurements are restricted to

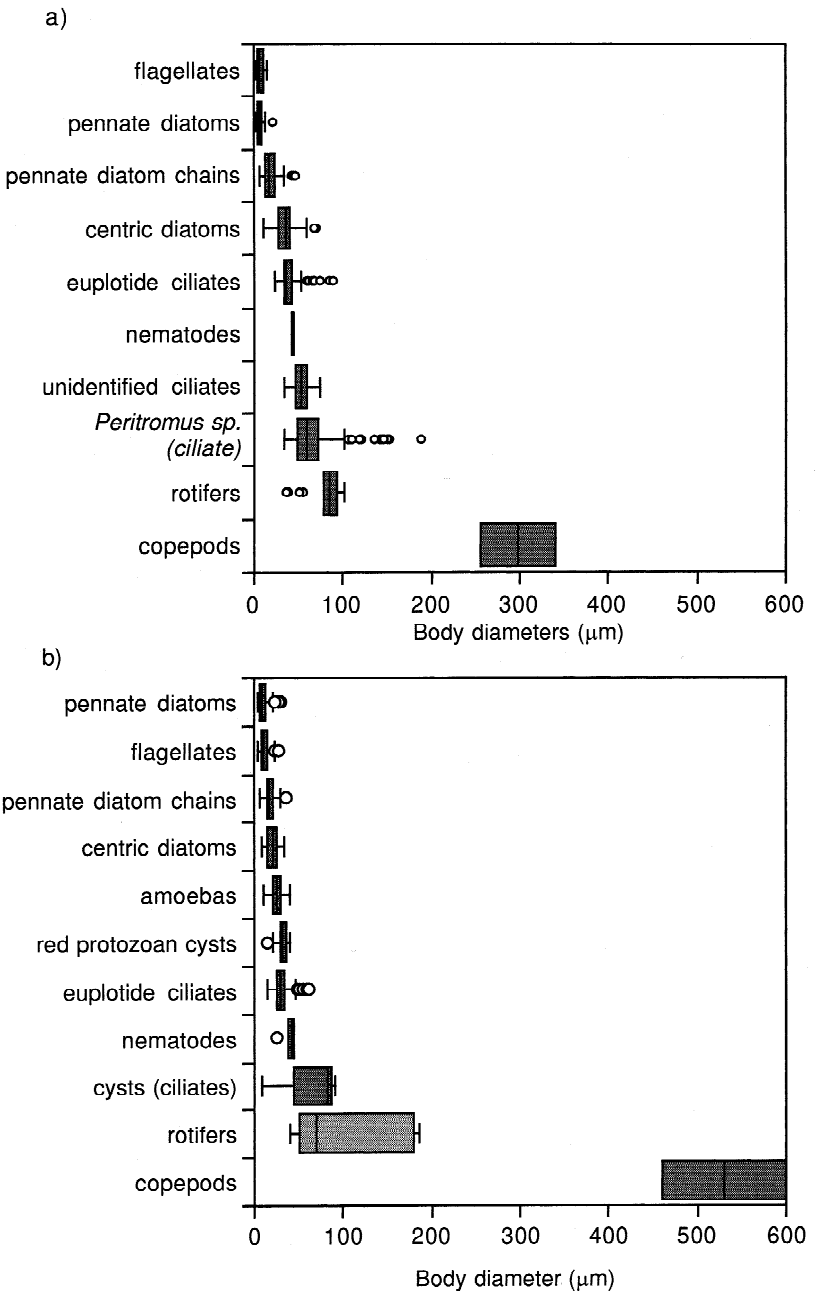

Fig. 8. Body diameter of organisms in the mixed cultures from the Laptev Sea in (a) 1995 and (b) 1996.

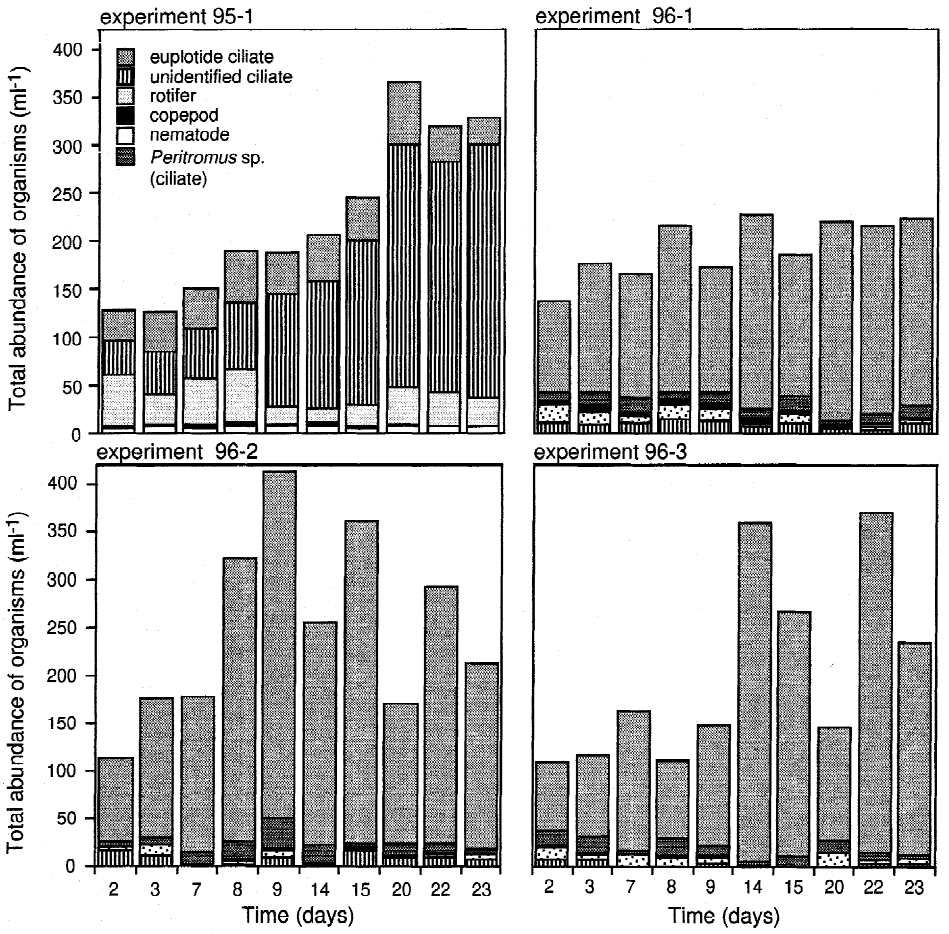

Fig. 9. Change in the total abundance of larger organisms taxa during the 23 day incubation inside the culture dish.

laboratory conditions due to three limitations: (1) freezing rates of the ice have to be known; (2) RC has to be added prior to freezing; and (3) RC also adsorbs to organic matter. Since small portions of the brine remain in the ice during the centrifugation process (see also Weissenberger et al., 1992) our measurements constitute conservative estimates which integrate surfaces of interconnected channel passages over larger volumes of ice.

The observed high variability of surface areas can partially be attributed to inaccuracies in the measurement of small brine volumes at high salinities and/or an intrinsic natural variability of the brine channel network. The different bulk salinities of the two ice types studied were comparable to natural sea ice (Eicken, 1992) and stayed within the range of new ice (Gradinger and Ikävalko, 1998). Our data do not allow a direct comparison of surface areas of both ice types due to the difference in bulk salinity.

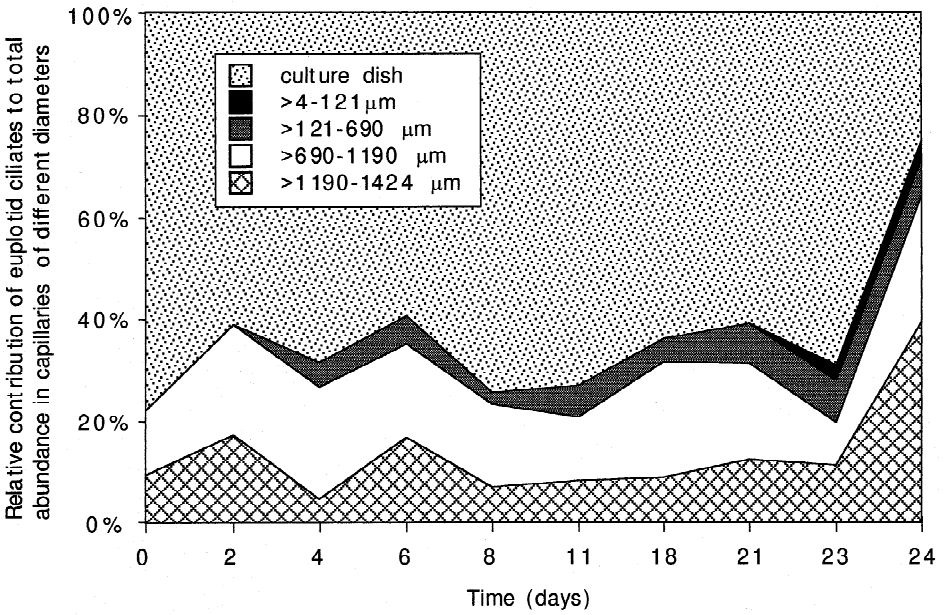

Fig. 10. Example of the change in the relative abundances of larger organism taxa during the 23 day incubation in different size capillaries and the culture dish.

But we infer that connectivity of pore space sensitively influences the internal surface area of sea ice (Fig. 14), even amongst ice of identical brine channel diameter frequencies, bulk salinity and temperature.

Detailed analyses of surface area in relation to pore channel volume, size, connectivity and biological accessibility of porous media are scarce and exist mainly for soils and the aquatic benthos. Consequently, we compare our data with those from terrestrial and aquatic sediments. The entire surface area (0.6–7 m^2 kg^{-1} ice) of the two ice types at approx. -2.5°C is one to two orders of magnitude lower than that of sand (Doeglas, 1968). However, the density of sediment is more than twice as high as that of ice. If surface area is related only to substratum volume, sandy soils and sea ice are very similar: columnar ice has surface areas of sand of 0.8 mm grain diameter, granular ice of sand of 6 mm. Such comparisons, however, ignore a fundamental difference in accessibility of surfaces by organisms, which is determined by the geometric dimensions of the brine channel system. Bulk porosity is of little significance to the organisms and so is permeability often used in marine sediment studies because both parameters do not describe the wide range of pore spaces that organisms encounter during their lives in marine ice (Freitag and Eicken, personal communication).

The data from our capillary experiment demonstrate that colonisation of the ice largely depends on the structure of the brine channel network. Similar observations were made for marine sediments (Jansson, 1967; Fenchel, 1969) where ciliates dominate the community in fine-grained sediment (200–120 µm), nematodes constitute the bulk metabolism in sand finer than 100 µm, while other meiofauna taxa (harpacticoid

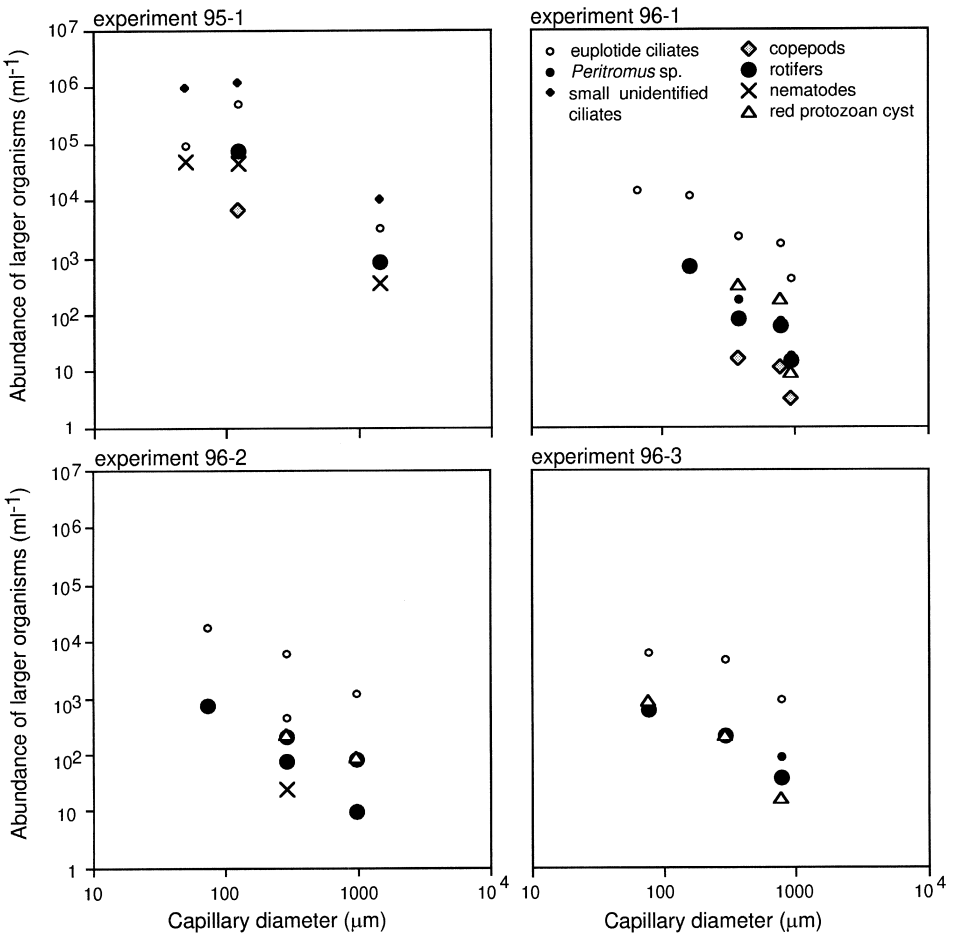

Fig. 11. Average abundances of larger organisms within different size capillaries during the 23 day incubation.

copepods, ostracods, rotifers) dominate the coarse sediment. The complexity of the brine channel system with half of the brine channels being smaller than 200 μm provides a multitude of spatial niches where organisms are freed from the grazing pressure of larger predators. Our results are in accordance with the 'critical pore sizes' determined for marine sediments (Patterson et al., 1989). Based on our experiments we speculate to find a shifted Sheldon spectrum (Sheldon et al., 1972; Schwinghamer, 1981) with higher proportions of larger predators in ice with larger brine channel diameters, but identical bulk parameters.

Flexible or elongated bodies are suited to traverse obstructing narrow passages and are thus typical for benthic meiofauna (Patterson et al., 1989) and sea ice biota. In our experiment, larger predators increased in abundance in small capillaries to the limit set by the diameter of the capillary. The high food concentrations located in very small channels likely challenged predators to access these sites. Traversing of narrow porous

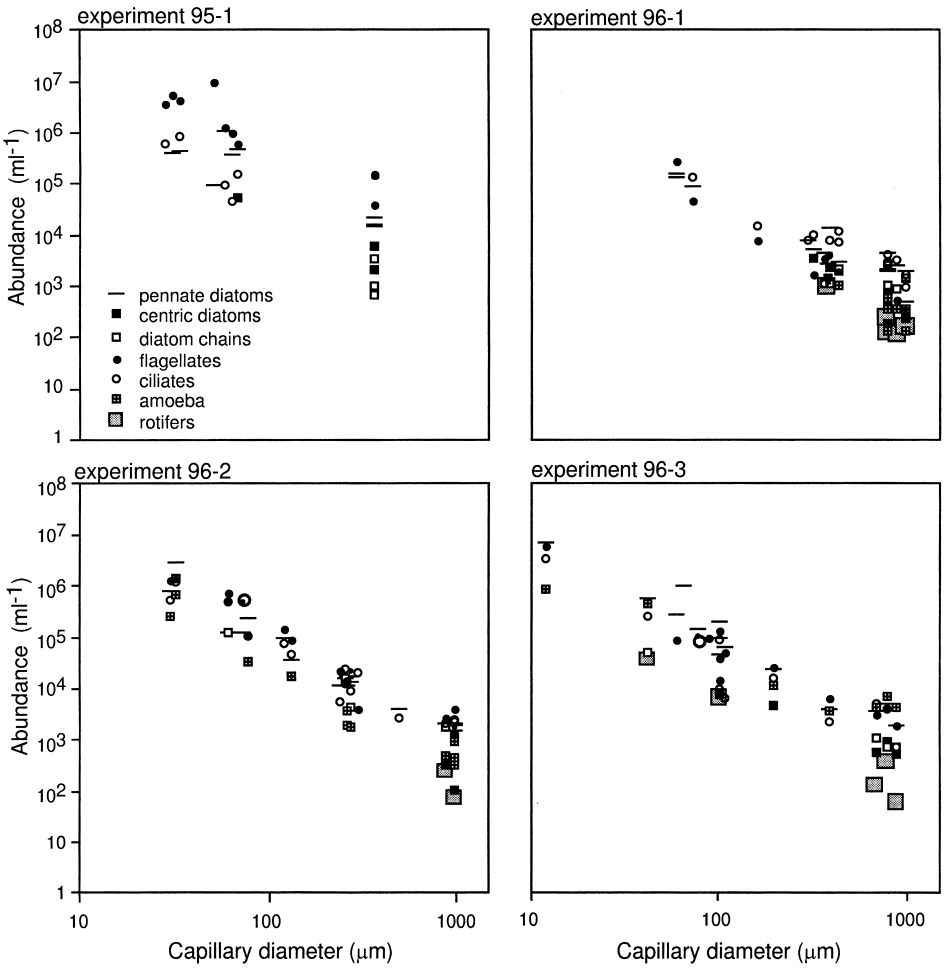

Fig. 12. Abundances of all organisms within different size capillaries after the 23 day incubation.

Table 2
Minimum capillary diameter traversed by sympagic ciliates and metazoans

Organism	Capillary diameter[a]
Euplotide ciliates	100
Rotifers	57
Turbellaria	60
Harpacticoid copepods	100
Amphipods	100

[a] Expressed as percent of the unflexed body diameter of the animal (%).

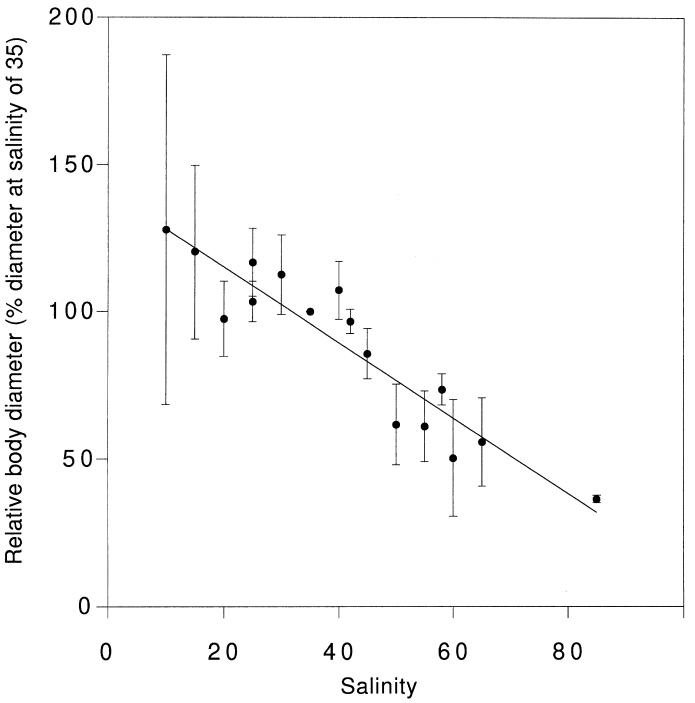

Fig. 13. Decrease in body diameter of turbellaria with increasing salinity.

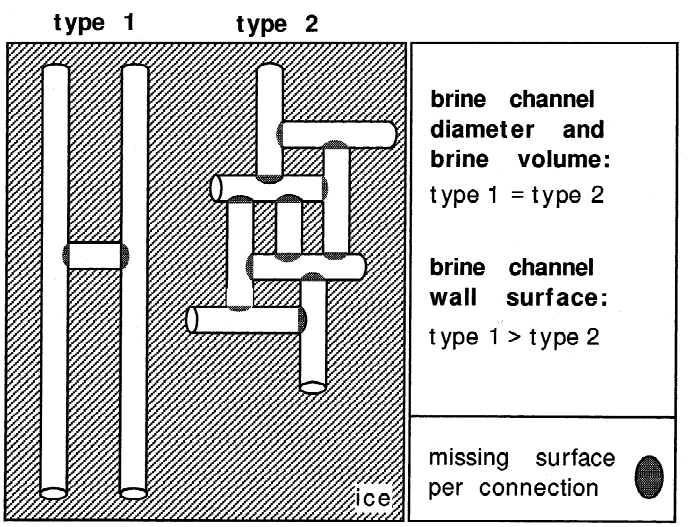

Fig. 14. Schematic representation of columnar and granular ice with identical bulk parameters and brine channel diameters. Internal surface reduction takes place by elevated interconnectivity of single-channel passages.

media favours locomotory organelles that are flexible and also function in deformed individuals: flagella, cilia, cirries and flexing of the entire body are found in most of the motile sympagic organisms (e.g., flagellates, ciliates, rotifers, nematodes, turbellaria; Gradinger et al., 1991)

Typical metazoan inhabitants of Arctic sea ice include very different morpho-types spanning from acoel turbellaria, nematodes to crustaceans. We observed that harpacticoid copepods entered narrow passages with sizes similar to their body diameters, whereas larger amphipods (*Apherusa glacialis*) avoided narrow passages. Turbellaria lack rigid morphological features, which makes them extremely plastic while traversing thin crevices. By also conforming to the osmotic pressure of the brine, turbellaria match their body dimensions to the fluctuating dimensions of the brine channel system during changes in temperature and salinity. Rotifers demonstrated an astonishing capacity to penetrate very narrow cylindrical long passages (several times their body length and 57% their body diameter). Such flexibility and their comparatively small size and good swimming ability should allow access to cavities in the network that are inaccessible to turbellaria. Although nematodes have a thin body dimension, their sporadic presence in small capillaries and their preference for organic aggregates suggests that they do not prefer small brine channels. Thin long bodies have been suggested to prevent wash-out in aquatic sediments (Patterson et al., 1989) and facilitate feeding in narrow passages in which they compete with or feed on micrograzers. We speculate that nematodes should therefore favour transitions between large and small channels. Ciliates with flattened body geometries and ventral oriented cilia, however, appear to access the majority of spaces.

Our brine channel frequency measurements suggest that the pore space ($\leq$200 μm) of sea ice constitutes a refuge in which bacteria, flagellates and pennate diatoms and small ciliates benefit from a reduced grazing pressure from metazoans. Approximately 50% of the entire internal surface of sea ice is allotted to brine channels of $<$41 μm. From our capillary experiments we infer that small brine channels should solely be colonised by the microbial community with concentrations one to two magnitudes higher than in the remaining brine channel network. A similar observation was made in soils, where minimum neck diameters of 4 μm for protozoa and 30 μm for nematodes have been suggested (Jones and Thomasson, 1976; Elliott et al., 1980), which reduced the pore volume accessible to protozoa and nematodes to less than 10% in a loamy soil. Minimal required dimensions of the brine channel system for identical taxa inhabiting the ice are comparable to soil, however the majority of space still remains accessible for most of the organisms of sea ice.

Conclusively, ice in its textural structure comprises sites of altered species composition related to the geometries of the substrate via the exclusion of larger organisms. Temperature, bulk salinity and ice texture, therefore, influence the predatory–prey interactions by superimposing its structural component on the dynamic of the sympagic food web. Despite the advantage of refuge space, small channels are unfavourable for the diffusive transport of vital molecules. Competition for shelter space for attached organisms therefore appears important in the vicinity of larger channels where, for example, nutrients can be replenished rapidly (Cota et al., 1991; Gradinger et al., 1992). The majority of the space inside the ice is accessible to organisms and 6–41% of the

Table 3
Estimated percent coverage of accessible internal ice surface by sympagic organisms from the Laptev Sea (Krembs and Engel, 1999) in granular and columnar ice of approx. −2 to −6°C

Organism group	Granular ice		Columnar ice	
	(−2°C)	(−6°C)	(−2°C)	(−6°C)
Diatoms	38	60	5	42
Ciliates	0.66	0.85	0.09	0.72
Heterotrophic flagellates	1	2	0.2	1.2
Phototrophic flagellates	0.7	1.2	0.10	0.81
Bacteria	0.13	0.20	0.10	0.14
Turbellaria	0.08	0.04	0.01	0.08
Copepods	0.27	0.12	0.03	0.30
Rotifers	0.0004	0.0004	0.0001	0.0005
Coverage (total)	41	64	6	46

brine network surface area at −2°C may be covered by microorganisms, mainly by diatoms (Table 3; Krembs, in preparation). The surface in granular ice might be more densely covered with organisms than in columnar ice with consequences for interspecific interactions. Compared with soils, where less that 1% of the total surface area (Adu and Oades, 1978; Jenkinson and Ladd, 1981) is covered by micro-organisms, the surface of ice crystals is colonised by higher fractions. Cooling from −2 to −6°C drastically increases the coverage of organisms due to surface reduction by approximately one order of magnitude.

In this article we stress the influence of brine channel geometry on the food-web relations. Bacteria are important as microbial mediators of decomposition processes and are significant for the overall geochemical cycling inside the ice (Kottmeier and Sullivan, 1988; Grossmann and Dieckmann, 1994; Gradinger and Zhang, 1997). Bacteria within soil aggregates exist in pores at least three times their diameter (Kilbertus, 1980), rendering 95% of the pore space in soil inaccessible; in contrast to soils, nearly the entire pore space in ice is accessible to bacteria. Future detailed field investigations on the distribution of bacteria and other organisms inside sea ice are needed to clarify the effect of ice texture on the geochemical cycle inside the ice matrix.

Acknowledgements

This work was supported by the Deutsche Forschungsgemeinschaft (Sp 377/4). We thank H. Eicken and J. Freitag for their technical and personal support.

References

Adu, J.K., Oades, J.M., 1978. Physical factors influencing decomposition of organic materials in soil aggregates. Soil Biol. Biochem. 10, 109–115.

Agatha, S., Wilbert, N., Spindler, M., Elbrächter, M., 1990. Euplotide ciliates in sea ice of the Weddell Sea (Antarctica). Acta Protozool. 29 (3), 221–228.

Alongi, D.M., 1987. The distribution and composition of deep-sea microbenthos in a bathyal region of western Coral Sea. Deep-Sea Res. 34, 1245–1254.

Andriashev, A.P., 1968. The problem of the life community associated with the Antarctic fast ice. In: Currie, R.I. (Ed.), Symposium on Antarctic Oceanography, Scott Polar Research Institute, Cambridge, pp. 147–155.

Assur, A., 1958. Composition of sea ice and its tensile strength. Nat. Res. Council Publ. 598, 106–138.

Carey, A.G., 1985. Marine ice fauna: Arctic. In: Horner, R. (Ed.), Sea Ice Biota, CRC Press, Boca Raton, FL, pp. 173–190.

Cota, G.R., Horne, E.P.W., 1989. Physical control of Arctic ice algal production. Mar. Ecol. Prog. Ser. 52, 111–121.

Cota, G.F., Legendre, L., Gosselin, M., Ingram, R.G., 1991. Ecology of bottom ice algae: I. Environmental controls and variability. J. Mar. Syst. 2, 257–278.

Cota, G.F., Prinsenberg, S., Bennett, E.B., Loder, J.W., Lewis, M.R., Anning, J.L., Watson, N.H.F., 1987. Nutrient fluxes during extended blooms of Arctic ice algae. J. Geophys. Res. 92 (C2), 1951–1962.

De Flaun, M.F., Mayer, L.M., 1983. Relationships between bacteria and grain surfaces in intertidal sediments. Limnol. Oceanogr. 28, 873–881.

Doeglas, D.J., 1968. Grain size indices, classification and environment. Sedimentology 10, 83–100.

Eicken, H., 1992. The role of sea ice in structuring Antarctic ecosystems. Polar Biol. 12, 3–13.

Eicken, H., Lensu, M., Leppäranta, M., Tucker, W.B., Gow, A.J., Salmela, O., 1995. Thickness, structure, and properties of level summer multi year ice in the Eurasian sector of the Arctic Ocean. J. Geophys. Res. 100, 22,697–22,710.

Elliott, E.T., Anderson, R.V., Coleman, D.C., Cole, C.V., 1980. Habitable pore space and microbial trophic interactions. Oikos 35, 327–335.

England, L.S., Hung, L., Trevors, J.T., 1993. Bacterial survival in soil: effect of clays and protozoa. Soil Biol. Biochem. 25, 525–531.

Fang, L.J., Cheung, F.B., Linehan, J.H., Pedersen, D.R., 1984. Selective freezing of a dilute salt solution on a cold ice surface. ASME J. Heat Transfer 106, 385–393.

Fenchel, T., 1969. The ecology of marine microbenthos IV: Structure and function of the benthic ecosystem, its chemical and physical factors and the microfauna communities with special reference to the ciliated protozoa. Ophelia 6, 1–182.

Frankenstein, G., Garner, R., 1967. Equations for determining the brine volume of sea ice from −0.5°C to −22.9°C. J. Glaciol. 6, 943–944.

Gradinger, R., Spindler, M., Henschel, D., 1991. Development of Arctic sea-ice organisms under graded snow cover. Polar Res. 10, 295–308.

Gradinger, R., Spindler, M., Weissenberger, J., 1992. On the structure and development of Arctic pack ice communities in Fram Strait: a multivariate approach. Polar Biol. 12, 727–733.

Gradinger, R., Zhang, Q., 1997. Vertical distribution of bacteria in Arctic sea ice of the Barents and Laptev Sea. Polar Biol. 17, 448–454.

Gradinger, R., Ikävalko, J., 1998. Organism incorporation into newly forming Arctic sea ice in the Greenland Sea. J. Plankton Res. 20, 871–886.

Grossmann, S., Dieckmann, G.S., 1994. Bacterial standing stock, activity, and carbon production during formation and growth of sea ice in the Weddell Sea, Antarctica. Appl. Environ. Microbiol. 60, 2746–2753.

Horner, R., 1985. Sea Ice Biota, CRC Press, Boca Raton, FL, 215 pp.

Horner, R., 1990. Ice-associated ecosystems. In: Medlin, L.K., Priddle, J. (Eds.), Polar Marine Diatoms, British Antarctic Survey, Cambridge, pp. 9–14.

Horner, R., Ackley, S.F., Dieckmann, G.S., Gulliksen, B., Hoshiai, T., Legendre, L., Melnikov, I.A., Reeburgh, W.S., Spindler, M., Sullivan, C.W., 1992. Ecology of sea ice biota. 1. Habitat, terminology, and methodology. Polar Biol. 12, 417–427.

Ikävalko, J., Gradinger, R., 1997. Flagellates and heliozoans in the Greenland Sea ice studied alive using light microscopy. Polar Biol. 17, 473–481.

Jansson, B.O., 1967. The significance of grain size and pore water content for the interstitial fauna of sandy beaches. Ophelia 4, 173–201.

Jenkinson, D.S., Ladd, J.N., 1981. Microbial biomass in soil: measurement and turnover. In: Paul, E.A., Ladd, J.N. (Eds.), Soil Biochem. 5, 415–471.

Jones, F.G.W., Thomasson, A.J., 1976. Bulk density as an indicator of pore space in soils usable by nematodes. Nematologica 22, 133–137.

Kilbertus, G., 1980. Etudes des microhabitats contenus dans les agregats du sol, leur relation avec la biomasse bacterienne et la taille des procaryotes presents. Rev. Ecol. Biol. Sol. 17, 545–557.

Krembs, C., Engel, A., 1999. Microorganisms, and TEP across the ice–water interface of melting first-year sea-ice in the Laptev Sea (Arctic) (in preparation).

Kottmeier, S.T., Sullivan, C.W., 1988. Sea ice microbial communities (SIMCO). 9. Effects of temperature and salinity on rates of metabolism and growth of autotrophs and heterotrophs. Polar Biol. 8, 293–304.

Lange, M.A., Eicken, H., 1991. Textural characteristics of sea ice and the major mechanisms of ice growth in the Weddell Sea. Ann. Glaciol. 15, 210–215.

Leppäranta, M., Manninen, T., 1988. The brine and gas content of sea ice with attention to low salinities and high temperatures. Finnish Institute of Marine Research, Internal Report, pp. 1–14.

Lighthart, B., 1969. Planktonic and benthic bacteriovorous protozoa at eleven stations in Puget Sound and adjacent Pacific Ocean. J. Fish. Res. Bd. Can. 26, 299–304.

Martin, S., 1981. Frazil ice in rivers and oceans. Annu. Rev. Fluid Mech. 13, 379–398.

Maykut, G.A., 1985. The ice environment. In: Horner, R. (Ed.), Sea Ice Biota, CRC Press, Boca Raton, FL, pp. 21–82.

Menge, B., Lubchenco, J., Ashkenas, L., 1985. Diversity, heterogeneity and consumer pressure in a tropical rocky intertidal community. Oecologia 65, 394–405.

Patterson, P., Larson, J., Corliss, J.O., 1989. The ecology of heterotrophic flagellates and ciliates living in marine sediments. Prog. Protistol. 3, 185–277.

Paul, V., Snelgrove, R., Butman, C.A., 1994. Animal–sediment relationships revisited: cause versus effect. Oceanogr. Mar. Biol. Annu. Rev. 32, 111–177.

Penzlin, H. (Ed.), 1981. Lehrbuch der Tierphysiologie, Gustav Fischer, pp. 310–312.

Schwinghamer, P., 1981. Characteristic size distribution of integral benthic communities. Can. J. Fish. Aquat. Sci. 38, 1255–1263.

Sheldon, R.W., Prakash, A., Sutcliffe, Jr. W.H., 1972. The size distribution of particles in the ocean. Limnol. Oceanogr. 17, 327–340.

Smiles, D.E., 1988. Aspects of the physical environment of soil organisms. Biol. Fertil. Soils 6, 204–215.

Smith, R.E.H., Clement, P., Cota, G.F., 1989. Population dynamics of bacteria in Arctic sea ice. Microb. Ecol. 17, 63–76.

Soane, B.D., Dickson, J.W., Campbell, D.J., 1982. Compaction by agricultural vehicles: a review. III. Incidence and control of compaction in crop production. Soil Tillage Res. 2, 3–36.

Spindler, M., Dieckmann, G.S., 1986. Distribution and abundance of the planktic foraminifer *Neogloboquadrina pachyderma* in sea ice of the Weddell Sea (Antarctica). Polar Biol. 5, 185–191.

Spindler, M., Dieckmann, G.S., Lange, M.A., 1990. Seasonal and geographic variations in sea ice community structure of the Weddell Sea, Antarctica. In: Kerry, K.R., Hempel, G. (Eds.), Ecological Change and Conservation, Springer, Berlin, pp. 129–135.

Sullivan, C.W., Palmisano, A.C., 1984. Sea ice microbial communities: distribution, abundance, and diversity of ice bacteria in McMurdo Sound, Antarctica, in 1980. Appl. Environ. Microbiol. 1984, 788–795.

Van Veen, J.A., Kuikman, P.J., 1990. Soil structural aspects of decomposition of organic matter by microorganisms. Biogeochemisty 11, 213–233.

Weissenberger, J., 1992. Die Lebensbedingungen in den Solekanälchen des antarktischen Meereises. Ber. Polarforsch. 111, 1–159.

Weissenberger, J., Dieckmann, G., Gradinger, R., Spindler, M., 1992. Sea ice: a cast technique to examine and analyse brine pockets and channel structure. Limnol. Oceanogr. 37, 179–183.

Yamamoto, N., Lopez, G., 1985. Bacterial abundance in relation to surface area and organic content of marine sediments. J. Exp. Mar. Biol. Ecol. 90, 209–220.